



# Hydrophilic Hyperbranched Polymer-Coated siRNA/Polyamidoamine Dendron-Bearing Lipid Complexes Preparation for High Colloidal Stability and Efficient RNAi

メタデータ	言語: eng 出版者: 公開日: 2021-04-23 キーワード (Ja): キーワード (En): 作成者: Yuba, Eiji, Korenaga, Takashi, Harada, Atsushi メールアドレス: 所属:
URL	<a href="http://hdl.handle.net/10466/00017383">http://hdl.handle.net/10466/00017383</a>

1 **Hydrophilic hyperbranched polymer-coated siRNA/polyamidoamine dendron-**  
2 **bearing lipid complexes preparation for high colloidal stability and efficient RNAi**

3

4 **Eiji Yuba<sup>1, \*</sup>, Takashi Korenaga<sup>1</sup>, Atsushi Harada<sup>1, \*</sup>**

5 <sup>1</sup> Department of Applied Chemistry, Graduate School of Engineering, Osaka Prefecture  
6 University, 1-1 Gakuen-cho, Naka-ku, Sakai, Osaka 5998531, Japan

7 \*Correspondence: yuba@chem.osakafu-u.ac.jp and harada@chem.osakafu-u.ac.jp

8 Tel.: +81-72-254-9330; Fax: +81-72-254-9330

9

10

11 **Abstract**

12 RNA interference (RNAi) using siRNA has gained much attention for use in therapies  
13 for cancer and genetic disorders. To establish RNAi-based therapeutics, the  
14 development of efficient siRNA nanocarriers is desired. Earlier, we developed  
15 polyamidoamine dendron-bearing lipids able to form complexes with nucleic acids as  
16 gene vectors. Especially, dendron lipids with unsaturated alkyl chains (DL-G1-U2)  
17 induced efficient endosomal escape by membrane fusion, leading to efficient  
18 transfection *in vitro*. For this study, dendron lipid having oleyl/linoleyl groups (DL-G1-  
19 U3) were designed to increase membrane fusogenic activity further. Indeed, DL-G1-  
20 U3/siRNA complexes achieved higher membrane fusogenic activity and knockdown of  
21 the target gene more efficiently than conventional DL-G1-U2/siRNA complexes did. A  
22 hydrophilic polymer, hyperbranched polyglycidol lauryl ester (HPG-Lau), was modified  
23 further on the surface of DL-G1-U3/siRNA complexes to provide colloidal stability.  
24 Surface modification of HPG-Lau increased the colloidal stability in a physiological  
25 condition more than complexes without HPG-Lau. Importantly, HPG-Lau-coated  
26 DL/siRNA complexes showed identical RNAi effects to those of parental DL/siRNA  
27 complexes, whereas RNAi activity of poly(ethylene glycol)-bearing lipid (PEG-PE)-  
28 modified DL/siRNA complexes was hindered completely. Introduction of unsaturated

29 bonds into dendron lipids and selection of suitable hydrophilic polymers for nanocarrier  
30 modification are important for obtaining efficient siRNA vectors towards *in vivo* siRNA  
31 delivery.

32

33 **Keywords:** dendron; siRNA; hyperbranched polymer; cationic lipid; membrane fusion

34

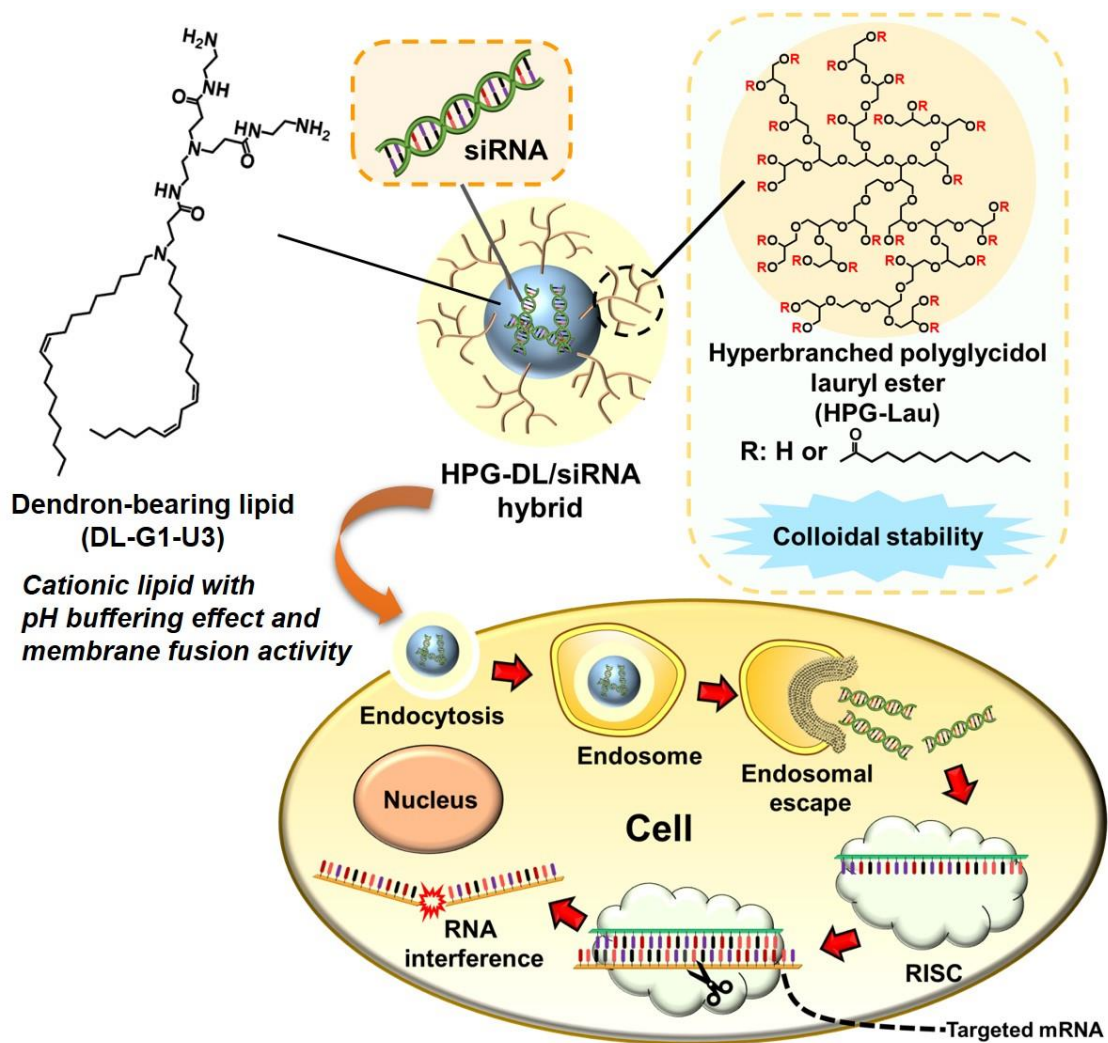
35 **Introduction**

36 RNA interference (RNAi), which inhibits specific gene expression using low-  
37 molecular double-stranded RNA, has gained much attention for application to cancer  
38 and genetic disorder therapies.<sup>1,2</sup> A representative RNA used for RNAi, siRNA  
39 suppresses specific gene expression by cutting the target mRNA. Unfortunately, RNase  
40 in the blood degrades siRNA easily. Furthermore, because siRNA has negative charge  
41 derived from phosphate groups of its backbone, the internalization of siRNA itself into  
42 cells is limited because of electrostatic repulsion with a negatively charged cell  
43 membrane.<sup>3,4</sup> Therefore, the development of delivery carriers able to prevent the  
44 degradation of siRNA and able to introduce siRNA into target cells is necessary. To  
45 date, siRNA delivery platforms of many types have been studied in both preclinical and  
46 clinical levels such as GalNAc-modified siRNA, cholesterol-conjugated siRNA, lipid  
47 nanoparticles containing siRNA, and polymer-siRNA complexes.<sup>5,6</sup> Among them,  
48 siRNA therapeutics of two types have been approved in a clinic: GalNAc-modified  
49 siRNA (Givosiran) and lipid nanoparticles containing siRNA (Patisiran) during the last  
50 two years.<sup>5,7,8</sup> However, target tissues or diseases of these approved siRNA therapeutics  
51 remain limited. Consequently, further improvement of siRNA delivery carriers is

52 necessary, such as selective delivery performance of siRNA into target cells, serum  
53 resistance, and colloidal stability in a physiological condition.

54 For earlier studies, polyamidoamine (PAMAM) dendron-bearing lipids were  
55 developed as plasmid DNA delivery vectors.<sup>9-12</sup> Dendron lipids were able to form  
56 complexes with nucleic acids via electrostatic interaction derived from primary amines  
57 in PAMAM dendron moiety. Dendron lipids achieved efficient endosomal escape  
58 further by pH-buffering effect derived from tertiary amines in dendron and membrane  
59 fusion activity of alkyl chains, resulting in efficient transfection.<sup>10, 12</sup> Moreover, various  
60 functionalities can be introduced to dendron lipids such as poly(ethylene glycol) (PEG)  
61 for biocompatibility and sugar moieties for targeting toward improvement of nucleic  
62 acid delivery performance.<sup>13, 14</sup> Considering these characteristics, the feasibility of  
63 dendron lipids for siRNA delivery platforms was investigated in this study. In an earlier  
64 report, dendron lipid having two oleyl chains (DL-G1-U2, Fig. S1a) exhibited efficient  
65 transfection activity by promotion of endosomal escape of pDNA via unsaturated alkyl  
66 chain-derived fusogenic activity.<sup>12</sup> Here, dendron lipids having oleyl/linoleyl chains  
67 (DL-G1-U3, Figure 1) were newly synthesized to increase membrane fusogenic activity  
68 further.

69 In an earlier report, introduction of PEG-modified dendron lipids to dendron lipid –  
70 nucleic acid complexes improved colloidal stability, although its transfection activity  
71 was reduced considerably.<sup>13</sup> In this study, to balance the colloidal stability and  
72 transfection activity, hyperbranched polyglycidol lauryl ester (HPG-Lau, Figure 1) was  
73 additionally modified to dendron lipid/siRNA complex surface as a hydrophilic polymer  
74 to shield the excess cationic charges and to provide the colloidal stability in a  
75 physiological condition. Here, the synthesis of DL-G1-U3, complex formation  
76 behaviors with siRNA, and siRNA delivery performance of dendron lipid/siRNA  
77 complexes with and without hydrophilic polymer coating were investigated.



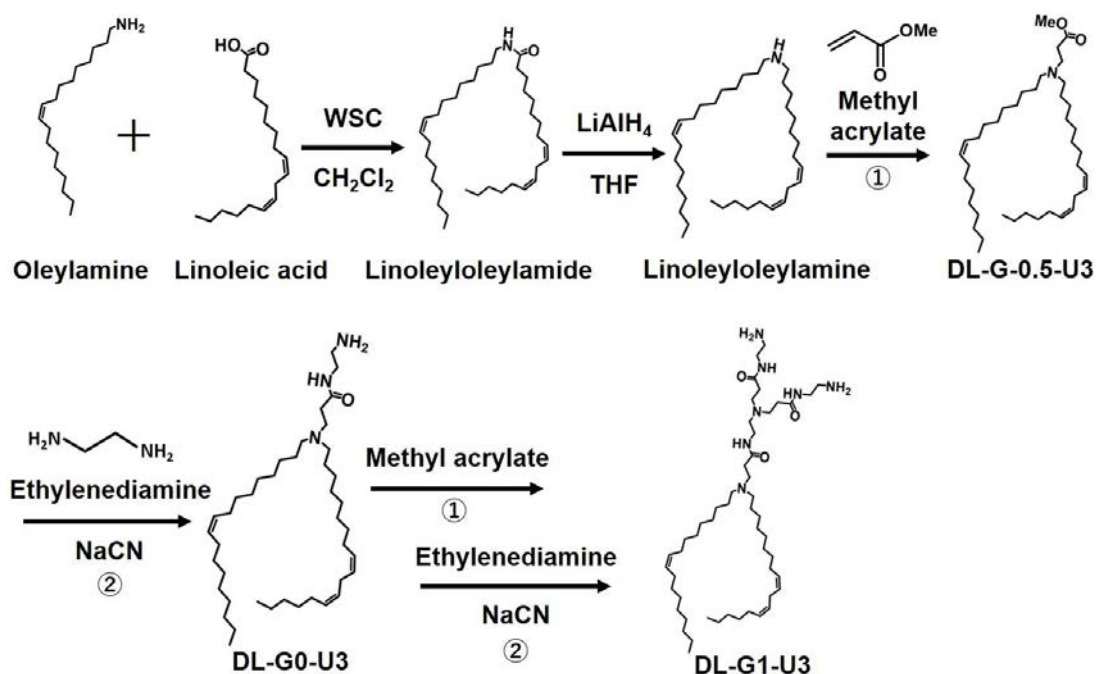
78

79 **Figure 1.** Design of polyamidoamine dendron-bearing lipid-siRNA complexes covered  
 80 with hydrophilic hyperbranched polymer (HPG-Lau) to provide colloidal stability and  
 81 promote endosomal escape of siRNA.

82

83 **Results and Discussion**

84           **Synthesis of dendron-bearing lipids.** For the synthesis of dendron-bearing  
 85 lipids having three unsaturated bonds in alkyl chains (DL-G1-U3), linoleyoleylamine  
 86 was prepared via condensation of oleylamine and linoleic acid, followed by reduction of  
 87 the amide group. Using a linoleyoleylamine as a starting material, the growth of  
 88 polyamidoamine dendron moiety was achieved via repeated Michael addition of methyl  
 89 acrylate and ester–amide exchange of ethylenediamine (Scheme 1). Synthesis of each  
 90 compound and the resultant DL-G1-U3 was confirmed using <sup>1</sup>H NMR and <sup>13</sup>C NMR, as  
 91 reported in *Supplementary information* and *Materials and Methods*. DL-G1-U2 was  
 92 also synthesized as reported earlier.<sup>12</sup>



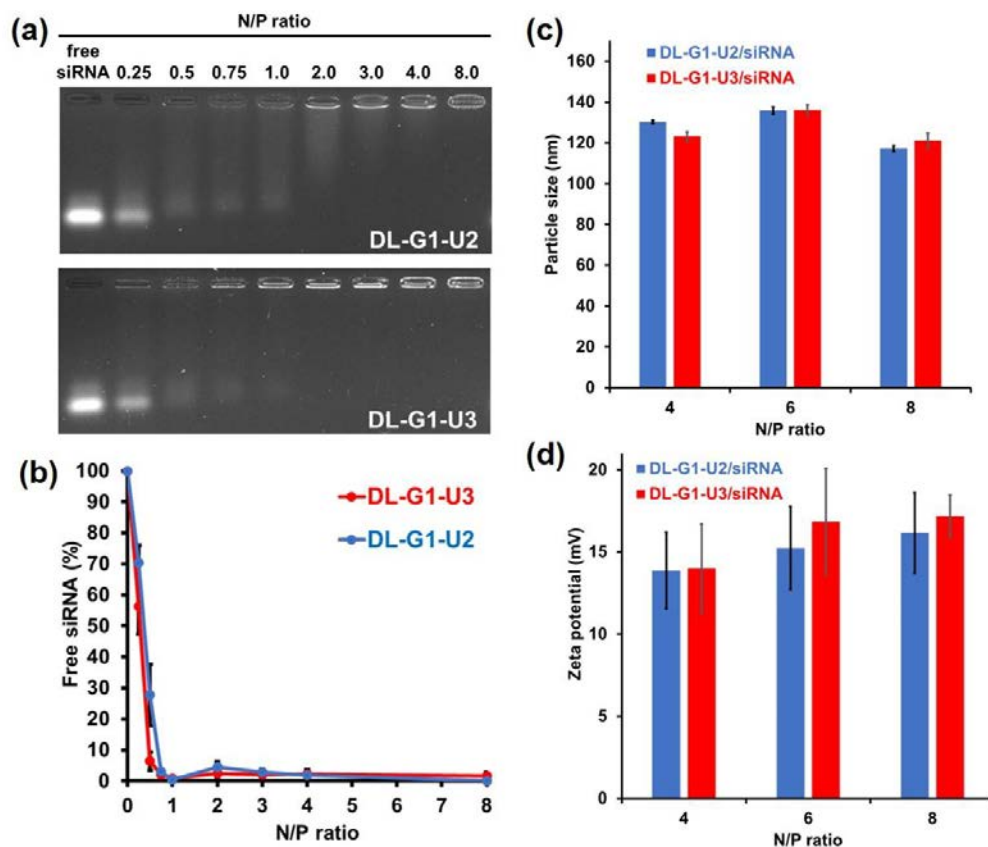
93

94

**Scheme 1.** Synthetic route for DL-G1-U3.

95

96           **Characterization of dendron lipid-siRNA complexes (lipoplexes).** Dendron  
97 lipid suspension was mixed with siRNA aqueous solution at varying charge ratios (N/P  
98 ratios). Then complex formation with siRNA was evaluated via electrophoretic analysis.  
99 With increase of the N/P ratio, free siRNA-derived fluorescence bands decreased;  
100 fluorescence was observed from the original point at above N/P ratio 2 (Fig. 2a).  
101 Remainder of the free siRNA fluorescence was determined quantitatively as presented  
102 in Fig. 2b. Free siRNA-derived fluorescence decreased drastically until N/P ratio of 1. It  
103 disappeared almost completely above N/P ratio 2. These results indicate that both DL-  
104 G1-U2 and DL-G1-U3 can form complexes (lipoplexes) with siRNA. No significant  
105 difference in complex formation behaviors between DL-G1-U2 and DL-G1-U3 was  
106 observed, indicating that complex formation with siRNA takes place mainly via  
107 electrostatic interaction between phosphate groups of siRNA and amines in a head  
108 group of both dendron lipids, as reported in dendron lipid/plasmid DNA complexes.<sup>9-12</sup>  
109 Complexes of DL-G1-U2/siRNA and DL-G1-U3/siRNA possessed around 120 nm size  
110 and cationic zeta potentials, as presented in Figs. 2c and 2d.



111

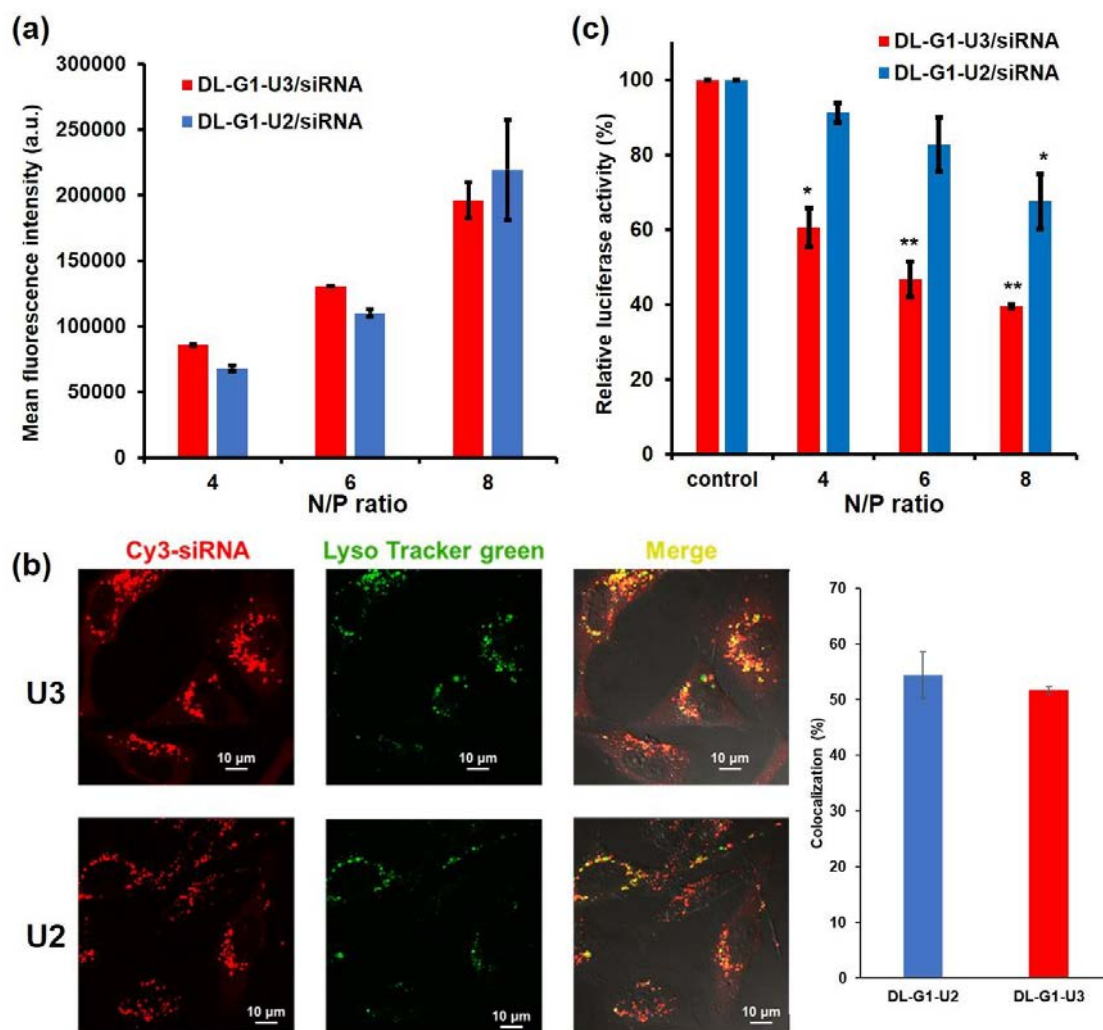
112 **Figure 2.** Agarose gel electrophoretic analysis of DL/siRNA complexes with various  
 113 N/P ratios (a). The percentage of free siRNA is shown against N/P ratios for  
 114 complexation of DL/siRNA (b). (c) Diameters and (d) zeta potentials of DL/siRNA  
 115 complexes at various N/P ratios.

116

117 **Cellular interaction and RNAi effect of lipoplexes.** Next, interaction of  
 118 lipoplexes with cells and RNAi effect were investigated. Before starting cell-related  
 119 evaluations, HeLa-Luc cells, stably luciferase-expressing cells, were treated with

120 varying siRNA dosages of lipoplexes to assess the cytotoxicity of the lipoplexes. As  
121 shown in Fig. S9a, no remarkable cytotoxicity was observed under 4-h sample  
122 incubation condition. Whereas lipoplexes with high N/P ratio induced significant  
123 decrease of cell viability under 24-h sample incubation condition (Fig. S9b). Therefore,  
124 the following experiments were performed by 4-h incubation. Figure 3a shows cellular  
125 fluorescence after 4-h incubation with lipoplexes containing FAM-labeled siRNA. With  
126 an increasing N/P ratio, FAM-siRNA uptake by HeLa-Luc cells increased, indicating  
127 that more cationic lipoplexes were taken up more efficiently by the cells. Figure 3b  
128 depicts intracellular distribution of Cy3-labeled siRNA delivered by DL-lipoplexes and  
129 colocalization evaluation with LysoTracker. Cells treated with DL-G1-U2/siRNA and  
130 DL-G1-U3/siRNA complexes show both dotted Cy3 fluorescence and diffused Cy3  
131 fluorescence within the cells, which respectively indicate siRNA trapped in  
132 endo/lysosomes and siRNA released in cytosol. According to results of quantitative  
133 analysis of colocalization, half of the Cy3 fluorescence was colocalized with  
134 LysoTracker Green fluorescence (Fig. 3b). Therefore, the remaining half of siRNA  
135 would be released from endo/lysosomes to cytosol. Figure 3c presents RNAi effects in  
136 HeLa-Luc cells treated with each complex. With increasing N/P ratios, the relative  
137 luciferase activity decreased, which corresponds to an increase in siRNA uptake with

138 N/P ratio increase (Fig. 3a). Furthermore, DL-G1-U3/siRNA complexes induced a  
 139 significantly higher RNAi effect than the DL-G1-U2/siRNA complex did (Fig. 3c). DL-  
 140 G1-U3/siRNA complex-treated cells show highly diffused Cy3 fluorescence within the  
 141 cells compared with DL-G1-U2/siRNA complex-treated cells (Fig. 3b). Such efficient  
 142 endosomal escape property of DL-G1-U3/siRNA complex might engender a strong  
 143 RNAi effect.



144

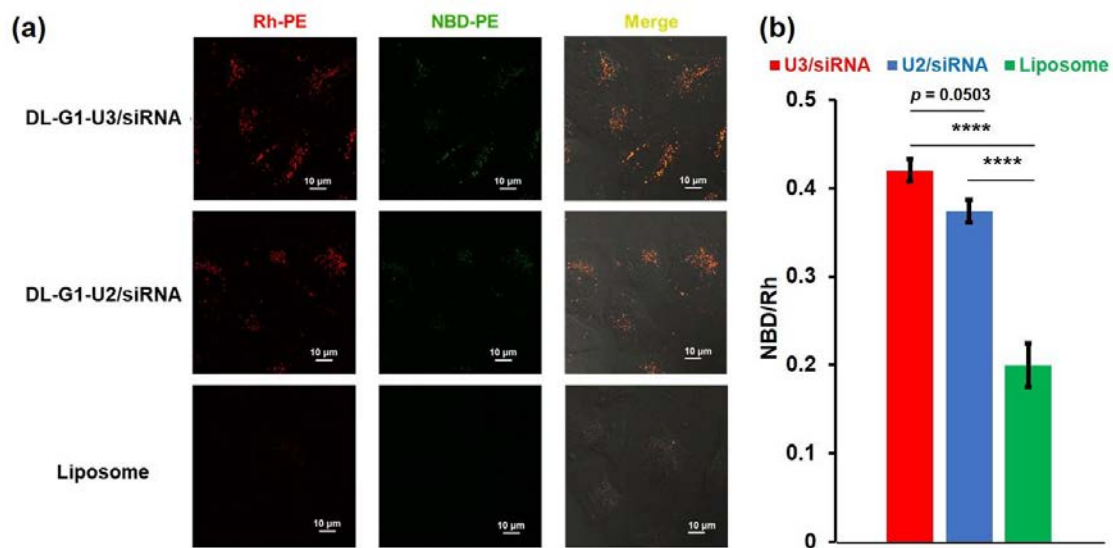
145 **Figure 3.** (a) Fluorescence intensity of HeLa-Luc cells treated with DL/FAM-siRNA  
146 complexes for 4 h. (b) Confocal laser scanning microscopic (CLSM) images of HeLa-  
147 Luc cell treated with DL/Cy3-siRNA complexes (N/P ratio 8) for 4 h. Intracellular  
148 acidic compartments were stained with LysoTracker Green. The co-localization  
149 coefficient for siRNA-derived fluorescence and LysoTracker Green fluorescence is also  
150 shown (right). (c) Relative luciferase activity of HeLa-Luc cells treated with DL/siRNA  
151 complexes in MEM with 10% serum. Cells were treated with the complexes for 4 h and  
152 were washed twice with PBS. After an additional 20 h culture, luciferase activity was  
153 evaluated. \* $P < 0.05$ ; \*\* $P < 0.01$  compared with the control group.

154

155 Fluorescence resonance energy transfer (FRET) analysis was conducted to  
156 confirm the endosomal escape properties of DL/siRNA complexes (Fig. 4).<sup>12,15</sup> After  
157 HeLa-Luc cells were treated with DL/siRNA complexes labeled with Rh-PE and NBD-  
158 PE, Rh fluorescence and NBD fluorescence within the cells were observed under  
159 excitation at 488 nm, which corresponds to the excitation wavelength of NBD. As a  
160 control, neutral liposome-treated cells showed very weak Rh fluorescence, whereas  
161 NBD fluorescence was difficult to detect, indicating that neutral liposomes exist as an  
162 intact state within the cells and indicating that Rh fluorescence was detected mainly via

163 FRET.<sup>16,17</sup> By contrast, DL/siRNA complex-treated cells showed not only Rh but also  
164 NBD fluorescence dots within the cells, suggesting that the recovery of NBD  
165 fluorescence took place via membrane fusion of lipoplexes with endosomal membrane,  
166 as reported earlier for DL/pDNA complexes.<sup>12</sup> Both DL/siRNA complexes have a  
167 significantly higher NBD/Rh ratio than those of neutral liposomes (Fig. 4b). In addition,  
168 DL-G1-U3/siRNA complexes show higher NBD/Rh ratios than those of DL-G1-  
169 U2/siRNA complexes ( $p = 0.0503$ ). Membrane fusion of lipoplexes is promoted by  
170 unsaturated alkyl chain-containing helper lipids such as dioleoyl  
171 phosphatidylethanolamine (DOPE).<sup>18,19</sup> Here, DL-G1-U3 includes three unsaturated  
172 bonds in its alkyl chains, whereas DL-G1-U2 includes two unsaturated bonds. More  
173 fluidic lipid membrane properties of DL-G1-U3-based lipoplexes might promote fusion  
174 with endosomal membrane, leading to cytosolic release of siRNA (Fig. 3b) and high  
175 RNAi effects (Fig. 3c).

176



177

178 **Figure 4.** (a) CLSM images of HeLa-Luc cells treated with DL/siRNA complexes or  
 179 EYPC liposomes containing 0.6 mol% of NBD-PE and Rh-PE for 4 h. NBD-PE and  
 180 Rh-PE fluorescence under excitation at 488 nm was observed using a CLSM. (b) Ratio  
 181 of NBD/Rh fluorescence found from CLSM images. \*\*\*\* $P < 0.0001$ .

182

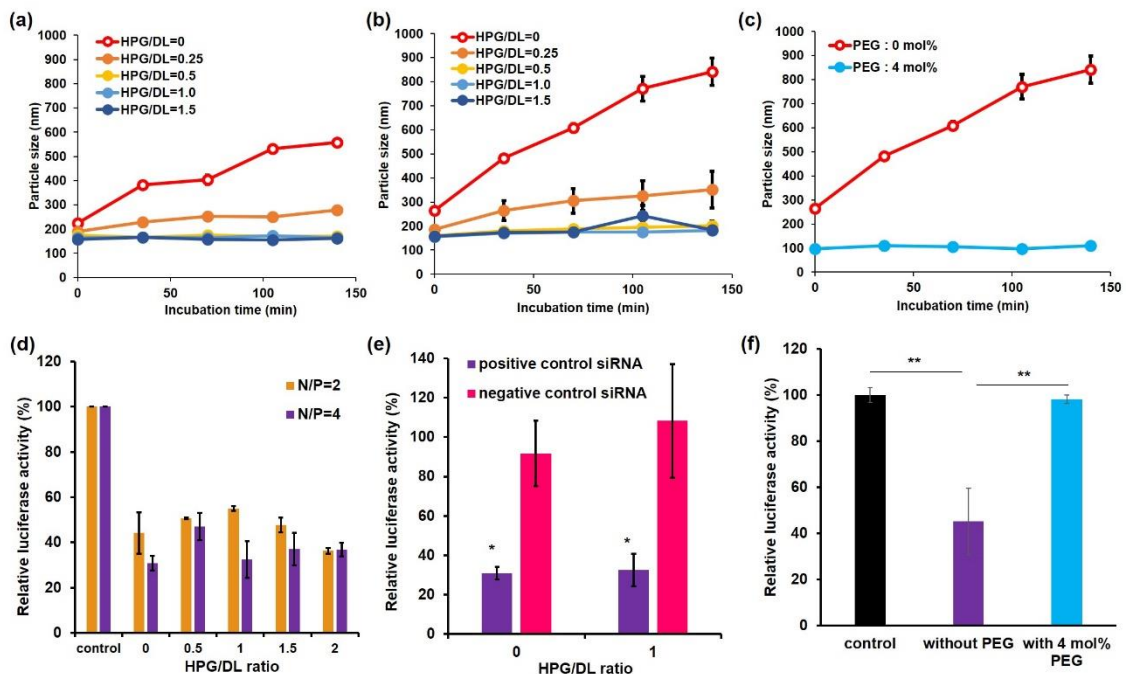
183 **Preparation of hydrophilic polymer-coated lipoplexes.** For application to *in vivo*  
 184 siRNA delivery, the colloidal stability of complexes in the biological fluids is a crucial  
 185 characteristic.<sup>20,21</sup> Therefore, the particle size change of DL/siRNA complexes in a  
 186 physiological condition was investigated (Fig. 5). Particle sizes of DL/siRNA  
 187 complexes in PBS increased with time. They reached 500–700 nm after 2 h incubation  
 188 (Figs. 5a and 5b), suggesting that DL/siRNA complexes tend to form aggregates

189 probably because electrostatic repulsion between cationic particles was cancelled in a  
190 physiological ionic strength condition.<sup>22,23</sup> To avoid such aggregation of DL/siRNA  
191 complexes, surface modification by hydrophilic polymers was performed. Here,  
192 hyperbranched polyglycidol lauryl ester (HPG-Lau) was coated onto DL/siRNA  
193 complexes via hydrophobic interaction of lauryl ester groups with complexes. After  
194 mixing of HPG-Lau at various weight ratios, the particle size change of hybrid  
195 complexes was evaluated. With increase of the HPG-Lau/DL ratio, aggregation of  
196 complexes was suppressed remarkably (Figs. 5a and 5b). When the HPG-Lau/DL ratio  
197 was greater than 0.5, the size of hybrid complexes was kept at an original particle size  
198 of less than 200 nm, which is a suitable size for enhanced permeation and retention  
199 effects or cellular uptake.<sup>24–27</sup> Considering that the zeta potentials of hybrid complexes  
200 slightly decreased concomitantly with the increase of HPG-Lau/DL ratio and the  
201 complexes still possessed a cationic charge at HPG-Lau/DL ratio 1.5 (Fig. S10), HPG-  
202 Lau might partly cover the surface of DL/siRNA complexes. The steric hindrance of  
203 hydrophilic hyperbranched polymers suppresses the aggregation of complexes in a  
204 physiological condition.<sup>28,29</sup> Such colloidal stability is also achievable by modification  
205 of 4 mol% (0.14 wt%) of linear hydrophilic polymer–lipid (PEG-PE) modification (Fig.  
206 5c).

207 Although HPG-Lau coating reduced the cytotoxicity of lipoplexes at high N/P  
208 ratios, 24-h incubation with complexes induced significant decrease of cell viability at  
209 N/P ratio 6 and 8 (Fig. S9b). Therefore, following cellular experiments were performed  
210 at N/P ratio 2 and 4. Figure S11 depicts the effects of HPG-Lau modification on cellular  
211 association and intracellular distribution of hybrid complexes. As shown in Fig. S11a,  
212 the siRNA uptake was unaffected by HPG-Lau modification, probably because hybrid  
213 complexes still have cationic zeta potentials even after modification of HPG-Lau (Fig.  
214 S10). As portrayed in Fig. S11b, the remarkable cytosolic delivery performance of  
215 DL/siRNA complexes was retained after HPG-Lau modification. Considering that  
216 HPG-Lau modification provides high colloidal stability to DL/siRNA complexes and  
217 reduction of cytotoxicity, RNAi effects on HeLa-Luc cells for lengthening of their  
218 incubation time (24 h) were evaluated (Fig. 5d). Compared with 4 h incubation results  
219 (Fig. 3c), knockdown effects of luciferase increased. Furthermore, hybrid complexes  
220 exhibited identical RNAi effects with DL/siRNA complexes without HPG-Lau  
221 modification. In addition, positive control (luciferase-specific) siRNA-containing  
222 complexes induced a significant decrease of relative luciferase activity of HeLa-Luc  
223 cells, although negative control (scramble) siRNA-containing complexes were unable to  
224 induce any RNAi effect (Fig. 5e), indicating that knockdown took place in a siRNA

225 sequence-specific manner. Results show that HPG-Lau modification can provide  
226 colloidal stability to DL/siRNA complexes without spoiling original biological activity.  
227 Also, PEG-PE-modified DL/siRNA complexes showed high colloidal stability at lesser  
228 amounts than HPG-Lau (Fig. 5c), whereas PEG-PE modification hindered RNAi effects  
229 of DL/siRNA complexes completely (Fig. 5f). PEG-PE is known to cover the 100 nm  
230 liposome surface sufficiently at greater than 2 mol% because of its high chain mobility  
231 and hydrophilic nature.<sup>30</sup> Such a hydrophilic layer formed by PEG might strongly  
232 suppress interaction with cells during entry into the cells and with the endosomal  
233 membrane, resulting in hindering of RNAi effects, as reported.<sup>31</sup> In the case of HPG-  
234 Lau modification, complete coverage of complex surfaces might be suppressed because  
235 of bulky hyperbranched structure of HPG, which is suggested from results of zeta  
236 potential change (Fig. S10). In addition, detachment of HPG-Lau might occur after  
237 internalization to the cells because HPG-Lau molecules were inserted onto the lipoplex  
238 membrane via single alkyl chain (lauryl ester), whereas PEG-PE molecules were  
239 incorporated tightly to DL lipid membrane via its phospholipid part. Such a difference  
240 in modification modes between PEG-PE and HPG-Lau might cause a difference in  
241 RNAi effect after modification onto DL/siRNA complexes. These results suggest the  
242 importance of hydrophilic polymer selection for nanocarrier surface modification to

243 provide both colloidal stability and nucleic acid delivery to target sites and cells. In the  
 244 case of PEG-modified nanoparticles, the detachment of PEG from nanoparticles at a  
 245 target site responding to pH or tumor-specific enzyme activity has been investigated to  
 246 promote internalization of nanoparticles to the target cells.<sup>32,33</sup> HPG-Lau can also be  
 247 introduced to such responsive properties by chemical modification of hydroxy groups to  
 248 adjust the detachment process precisely. By optimization of cationic lipid structures and  
 249 modification or detachment modes of hydrophilic polymers, efficient *in vivo* siRNA  
 250 nanocarriers can be designed to be stable in the bloodstream, accumulate to the target  
 251 site, and then induce strong RNAi effects.



252

253 **Figure 5.** Time courses of particle size changes of DL-G1-U3/siRNA-HPG hybrids (a)  
254 N/P=2 or (b) N/P=4 in PBS. (c) Time courses of particle size changes of DL-G1-  
255 U3/siRNA-PEG hybrids at N/P=4. (d) Relative luciferase activity of HeLa-Luc cells  
256 treated with HPG-DL-G1-U3/siRNA hybrids in MEM with 10% serum for 24 h  
257 (siRNA: 0.50  $\mu\text{g}/\text{well}$ ). (e) Relative luciferase activity of HeLa-Luc cells treated with  
258 HPG-DL-G1-U3 hybrids containing Luc-siRNA or scramble siRNA (N/P=4) for 24 h.  
259 (f) Relative luciferase activity of HeLa-Luc cells treated with DL-G1-U3/siRNA  
260 complexes with or without PEG-lipid (N/P=4) for 24 h. \* $P < 0.05$  compared with  
261 negative control groups; \*\* $P < 0.01$ .

262

## 263 **Conclusion**

264 For this study, a polyamidoamine dendron-bearing lipid having unsaturated alkyl  
265 chains (DL-G1-U3) was newly synthesized to promote endosomal escape of siRNA and  
266 to induce efficient RNAi. Results demonstrate that DL-G1-U3/siRNA complexes  
267 achieved high membrane fusogenic property and RNAi activity compared with  
268 conventional DL-G1-U2/siRNA complexes. Furthermore, hyperbranched polymer  
269 modification provided high colloidal stability without decreasing the original RNAi

270 activity of DL/siRNA complexes, whereas PEG-PE modification to DL/siRNA  
271 complexes completely hindered RNAi activity. Therefore, the increase of unsaturated  
272 bonds in the hydrophobic part of dendron-bearing lipids and selection of hydrophilic  
273 polymers are important to design efficient nucleic acid nanocarriers for *in vivo*  
274 application.

275

## 276 **Materials and Methods**

277 **Materials.** Egg yolk phosphatidylcholine (EYPC) and N-[methoxy (polyethylene  
278 glycol) 2000]-distearoyl phosphatidylethanolamine (PEG-PE) were kindly donated by  
279 NOF Co. (Tokyo, Japan). Hyperbranched polyglycidol lauryl ester (HPG-Lau, degrees  
280 of polymerization: 100, esterification%: 8%) was kindly donated by Daicel Corp.  
281 (Hiroshima, Japan). Oleylamine, linoleic acid and fetal bovine serum (FBS) were  
282 purchased from Sigma (St. Louis, MO.). Lithium aluminum hydride, sodium cyanide  
283 and 1-ethyl-3-(3-dimethylaminopropyl)carbodiimide, hydrochloride (WSC) were  
284 obtained from Wako Pure Chemicals Inc. (Osaka, Japan). Methyl acrylate and  
285 ethylenediamine were purchased from Nacalai tesque (Kyoto, Japan). 3-(4,5-Dimethyl-  
286 2-thiazolyl)-2,5-diphenyltetrazolium bromide (MTT) was obtained from Tokyo  
287 Chemical Industries Ltd. (Tokyo, Japan). N-(7-Nitrobenz-2-oxa-1,3-diazol-4-yl)-1,2-

288 dihexadecanoyl-*sn*-glycero-3-phosphoethanolamine (NBD-PE) and lissamine  
289 rhodamine B-sulfonyl phosphatidylethanolamine (Rh-PE) were purchased from Avanti  
290 Polar Lipids (Birmingham, AL, USA). AccuTarget™ Luciferase Positive Control  
291 siRNA was obtained from Bioneer Corp. (SP-3003, Daejeon, Republic of Korea).  
292 Universal negative control siRNA (21 mer), which has no homology for all genes of  
293 eukaryotes, and FAM- or Cy3-labeled universal negative control siRNA were purchased  
294 from Nippon Gene Co. Ltd. (Tokyo, Japan). Conventional polyamidoamine dendron-  
295 bearing lipid (DL-G1-U2, Fig. S1a) was synthesized as previously reported.<sup>12</sup>  
296 **Synthesis of DL-G1-U3.** A series of synthesis for linoleylolyleylamine and subsequent  
297 growth of dendron moiety until DL-G0.5-U3 was described in Supplementary  
298 information and each compound was characterized using <sup>1</sup>H NMR as shown in Figs.  
299 S2-S6. DL-G0.5-U3 (0.30 g, 0.36 mmol) dissolved in methanol (9.4 mL) was added to  
300 ethylenediamine (12 mL, 0.18 mol) containing sodium cyanide (6.9 mg, 0.14 mmol),  
301 and the mixed solution was stirred at 50°C for 48 h under nitrogen. The methanol and  
302 unreacted ethylenediamine were removed from the reaction mixture under vacuum. The  
303 crude product was dissolved in distilled water and dialyzed (MWCO: 1,000) against  
304 distilled water for 4 days and the DL-G1-U3 was recovered by lyophilization. The yield

305 was 0.27 g (85.4%),  $^1\text{H}$  NMR and  $^{13}\text{C}$  NMR for DL-G1-U3 were shown in Fig. S7 and  
306 Fig. S8, respectively.

307 **Preparation of lipoplexes.** PBS (pH was adjusted to 5.0) was added to a dry thin  
308 membrane of the dendron-bearing lipid. Solution was sonicated for 2 min using a bath-  
309 type sonicator to give a suspension of the dendron lipid. A given amount of siRNA was  
310 dissolved in 89 mM Tris, 89 mM boronic acid, and 2 mM EDTA aqueous solution (50  
311  $\mu\text{L}$ ), added to a given volume (0-50  $\mu\text{L}$ ) of the dendron lipid suspension, and incubated  
312 for 30 min at room temperature to afford a lipoplex with varying ratios of primary amino  
313 group of dendron lipids to siRNA phosphate (N/P ratios, N: primary amino group (mol)  
314 and P: phosphate (mol) were calculated from the concentrations of dendron lipid  
315 suspension and siRNA solution, respectively.).

316 **Agarose gel electrophoresis.** The lipoplexes consisting of dendron lipids were prepared  
317 by mixing siRNA (0.8  $\mu\text{g}$ ) dissolved in 89 mM Tris, 89 mM boronic acid, and 2 mM  
318 EDTA buffer (5  $\mu\text{L}$ ) and lipid suspension (5  $\mu\text{L}$ ). After 30 min-incubation at room  
319 temperature, the samples were mixed with 2.5  $\mu\text{L}$  of 65% sucrose, 89 mM Tris and 2 mM  
320 EDTA. Then, an aliquot of the samples (10  $\mu\text{L}$ ) was electrophoresed on 3.0 wt% agarose  
321 gel in 89 mM Tris, 89 mM boronic acid, and 2 mM EDTA aqueous solution (pH 8.0) with  
322 1  $\mu\text{g}/\text{mL}$  ethidium bromide at 100 V for 30 min. The ethidium bromide-stained bands

323 were visualized using a LAS-1000UVmini (Fujifilm, Japan) and analyzed with Science  
324 Lab 2003 Multi Gauge software (Fujifilm, Japan).

325 **Characterization of lipoplexes.** Diameters and zeta potentials of lipoplexes in 0.1 mM  
326 phosphate aqueous solution were measured using a Zetasizer Nano ZS (Malvern  
327 Instruments Ltd., Worcestershire, UK). Data were obtained as an average of more than  
328 three measurements on different samples.

329 **Cell viability.** HeLa-Luc cells, which are cell lines expressing luciferase stably, were  
330 seeded in 0.4 mL of MEM supplemented with 10% FBS in 48-well culture plates at  $2.9$   
331  $\times 10^4$  cells per well. After one day, the cells were washed with PBS containing 0.36 mM  
332  $\text{CaCl}_2$  and 0.42 mM  $\text{MgCl}_2$  (PBS(+)) and then MEM containing 10% FBS (0.18 mL) was  
333 added. Lipoplexes (20  $\mu\text{L}$ ) were gently applied to the cells and incubated for 4 h at 37°C.  
334 Then, the cells were rinsed with PBS(+), supplied with MEM containing 10% FBS, and  
335 incubated at 37°C. After 20 h, the cell viability was assessed by MTT assay.

336 **Cellular uptake.** HeLa-Luc cells ( $2.9 \times 10^4$  cells) cultured overnight in a 48-well plate  
337 were washed with PBS(+) and then incubated in culture medium. The lipoplexes  
338 containing FAM-siRNA were added gently to the cells and incubated for 4 h at 37°C. The  
339 cells were washed with PBS(+) three times, and then the detached cells using trypsin were  
340 applied to a flow cytometric analysis (CytoFlex, Beckman Coulter, Inc.).

341 **Intracellular distribution of lipoplexes.** HeLa-Luc cells ( $2 \times 10^5$  cells) cultured  
342 overnight in 35-mm glass-bottom dishes were washed with PBS(+), and then incubated  
343 in MEM containing 10% FBS (1900  $\mu$ L). The lipoplexes containing 1.5  $\mu$ g of Cy3-siRNA  
344 (100  $\mu$ L) were added gently to the cells and incubated for 4 h at 37°C. After the incubation,  
345 the cells were washed with PBS(+) three times. Confocal laser scanning microscopic  
346 (CLSM) analysis of these cells was performed using LSM 5 EXCITER (Carl Zeiss Co.  
347 Ltd.). Intracellular acidic organelles were also stained by LysoTracker Green (Invitrogen)  
348 according to manufacturer's instructions.

349 **RNA interference.** HeLa-Luc cells ( $2.9 \times 10^4$  cells) cultured overnight in a 48-well plate  
350 were washed with PBS(+) and then incubated in culture medium. The lipoplexes  
351 containing anti-luciferase siRNA (0.5  $\mu$ g) were added gently to the cells and incubated  
352 for 4 h at 37°C. The cells were washed with PBS(+) three times, and then supplied with  
353 MEM containing 10% FBS, and incubated at 37°C. After 24 h, the cells were lysed by  
354 adding 50  $\mu$ L of Luc-PGC-50 detergent (Toyo Ink, Japan). A 20  $\mu$ L aliquot from each  
355 sample was used for luciferase assay kit (Toyo Ink) and luciferase activities were  
356 analyzed using a Lumat LB9507 luminometer (Berthold, Bad Wildbad, Germany). The  
357 protein content of the lysate was measured by Coomassie Protein Assay Reagent (Pierce,  
358 IL) using bovine serum albumin as the standard.

359 **Analysis of intracellular fusion.** Lipoplexes containing NBD-PE and Rh-PE were  
360 prepared as described above except that mixtures of dendron lipids, NBD-PE (0.6 mol%)  
361 and Rh-PE (0.6 mol%) were dispersed in PBS. EYPC liposomes containing NBD-PE (0.6  
362 mol%) and Rh-PE (0.6 mol%) were also prepared as a negative control. HeLa-Luc cells  
363 ( $2 \times 10^5$  cells) cultured overnight in 35-mm glass-bottom dishes were washed with  
364 PBS(+), and then incubated in DMEM containing 10% FBS (1900  $\mu$ L). Then, the  
365 lipoplexes (1.5  $\mu$ g of siRNA, 100  $\mu$ L) or EYPC liposomes (0.1 mM lipids) were added  
366 gently to the medium of the cells and incubated for 4 h at 37°C. After the incubation, the  
367 cells were washed with PBS(+) three times and analyzed by CLSM. Fluorescence of  
368 NBD-PE and Rh-PE was observed through specific path filters ( $\lambda_{em}$ =500–530 nm for  
369 NBD-PE and  $\lambda_{em} > 560$  nm for Rh-PE) with excitation of NBD-PE at 488 nm.  
370 Fluorescence intensity ratios of NBD-PE to Rh-PE of these cells were also determined by  
371 LSM 5 EXCITER software.

372 **Preparation of hydrophilic polymer-coated lipoplexes.** HPG-Lau aqueous solution  
373 was added to freshly prepared lipoplexes at various weight ratios of HPG-Lau/dendron  
374 lipids and incubated for 30 min at room temperature. PEG-PE-coated lipoplexes was also  
375 prepared by incubation of lipoplexes with 4 mol% of PEG-PE aqueous suspension for 30  
376 min.

377 **Characterization of hydrophilic polymer-coated lipoplexes.** Diameter in PBS and zeta  
378 potentials of hydrophilic polymer-coated lipoplexes in 0.1 mM phosphate aqueous  
379 solution were measured using a Zetasizer Nano ZS. Data were obtained as an average of  
380 more than three measurements on different samples. Cellular uptake, intracellular  
381 distribution and RNAi effect of hydrophilic polymer-coated lipoplexes after 24 h  
382 incubation in culture medium were analyzed as same with described above.

383 **Statistical analysis.** Statistical analyses were performed using Prism (v8, GraphPad).  
384 When one-way ANOVA followed by Tukey's HSD post hoc test was used, variance  
385 between groups was found to be similar by Brown-Forsythe test. The symbols \*, \*\*,  
386 and \*\*\*\* indicate *P* values less than 0.05, 0.01 and 0.0001, respectively.

387

#### 388 **CRedit authorship contribution statement**

389 **Eiji Yuba:** Conceptualization, Project administration, Data curation, Funding  
390 acquisition, Writing - original draft, Writing - review & editing. **Takashi Korenaga:**  
391 Investigation, Methodology. **Atsushi Harada:** Funding acquisition, Supervision, Data  
392 curation, Writing - review & editing.

393

#### 394 **Supporting information**

395 The Supporting Information is available free of charge on the ACS Publications website  
396 at DOI: XXX.

397 Figures showing chemical structures of dendron lipids, synthetic procedures  
398 and characterization of linoleyloleamide, linoleyloleylamine and a series of  
399 dendron-bearing lipids, cytotoxicity of dendron lipid/siRNA complexes with or  
400 without HPG-Lau, zeta potentials, cellular uptake and intracellular distribution  
401 of HPG-Lau-coated dendron lipid/siRNA complexes.

402

#### 403 **Declaration of Competing Interest**

404 The authors declare no conflict of interest.

405

#### 406 **Acknowledgments**

407 This research was funded by Grants-in-aid for Scientific Research from the  
408 Ministry of Education, Science, Sports, and Culture in Japan, grant number  
409 (15H03024).

410 **References**

- 411 1. D. Bumcrot, M. Manoharan, V. Koteliansky, D.W.Y. Sah, RNAi therapeutics: a  
412 potential new class of pharmaceutical drugs, *Nat. Chem. Biol.* 2 (2006) 711-719.
- 413 2. R.L. Setten, J.J. Rossi, S.P. Han, The current state and future directions of RNAi-  
414 based therapeutics, *Nat. Rev. Drug Discov.* 18 (2019) 421-446.
- 415 3. D. Reischl, A. Zimmer, Drug delivery of siRNA therapeutics: potentials and limits  
416 of nanosystems, *Nanomedicine* 5 (2009) 8-20.
- 417 4. T. Tokatlian, T. Segura, siRNA applications in nanomedicine, *Wiley Interdiscip.*  
418 *Rev. Nanomed. Nanobiotechnol.* 2 (2010) 305–315.
- 419 5. B. Hu, L. Zhong, Y. Weng, L. Peng, Y. Huang, Y. Zhao, X.-J. Liang, Therapeutic  
420 siRNA: state of the art, *Signal Transduct. Target Ther.* 5 (2020) 101.
- 421 6. B. Hu, Y. Weng, X.-H. Xia, X.-J. Liang, Y. Huang, Clinical advances of siRNA  
422 therapeutics, *J. Gene Med.* 21 (2019) e3097.
- 423 7. S.M. Hoy, Patisiran: First Global Approval, *Drugs* 78 (2018) 1625-1631.
- 424 8. L.J. Scott, Givosiran: First Approval, *Drugs* 80 (2020) 335-339.
- 425 9. T. Takahashi, K. Kono, T. Itoh, N. Emi, T. Takagishi, Synthesis of novel cationic  
426 lipids having polyamidoamine dendrons and their transfection activity, *Bioconjug.*  
427 *Chem.* 14 (2003) 764-773.

- 428 10. T. Takahashi, C. Kojima, A. Harada, K. Kono, Alkyl chain moieties of  
429 polyamidoamine dendron-bearing lipids influence their function as a nonviral gene  
430 vector, *Bioconjug. Chem.* 18 (2007) 1349-1354.
- 431 11. K. Kono, R. Ikeda, K. Tsukamoto, E. Yuba, C. Kojima, A. Harada, Polyamidoamine  
432 dendron-bearing lipids as a non-viral vector: influence of dendron  
433 generation, *Bioconjug. Chem.* 23 (2012) 871-879.
- 434 12. E. Yuba, Y. Nakajima, K. Tsukamoto, S. Iwashita, C. Kojima, A. Harada, K. Kono,  
435 Effect of unsaturated alkyl chains on transfection activity of poly(amidoamine)  
436 dendron-bearing lipids, *J. Control. Release* 160 (2012) 552-560.
- 437 13. T. Takahashi, J. Hirose, C. Kojima, A. Harada, K. Kono, Synthesis of  
438 poly(amidoamine) dendron-bearing lipids with poly(ethylene glycol) grafts and their  
439 use for stabilization of nonviral gene vectors, *Bioconjug. Chem.* 18 (2007) 1163-  
440 1169.
- 441 14. T. Takahashi, E. Yuba, C. Kojima, A. Harada, K. Kono, Synthesis of a  
442 polyamidoamine dendron-bearing lipid having sugar moieties and its use for  
443 preparation of nonviral gene vectors, *Res. Chemical Intermediates* 35 (2009) 1005-  
444 1014.

- 445 15. S. Magalhães, S. Duarte, G.A. Monteiro, F. Fernandes, Quantitative evaluation of  
446 DNA dissociation from liposome carriers and DNA escape from endosomes during  
447 lipid-mediated gene delivery, *Hum. Gene Ther. Methods* 25 (2014) 303–313.
- 448 16. A. El-Sayed, I.A. Khalil, K. Kogure, S. Futaki, H. Harashima, Octaarginine- and  
449 octalysine-modified nanoparticles have different modes of endosomal escape, *J.*  
450 *Biol. Chem.* 283 (2008) 23450-23461.
- 451 17. E. Yuba, A. Harada, Y. Sakanishi, K. Kono, Carboxylated hyperbranched  
452 poly(glycidol)s for preparation of pH-sensitive liposomes, *J. Control. Release* 149  
453 (2011) 72-80.
- 454 18. I.S. Zuhorn, U. Bakowsky, E. Polushkin, W.H. Visser, M.C.A. Stuart, J.B.F.N.  
455 Engberts, D. Hoekstra, Nonbilayer phase of lipoplex-membrane mixture determines  
456 endosomal escape of genetic cargo and transfection efficiency, *Mol. Ther.* 11 (2005)  
457 801-810.
- 458 19. Z. Du, M.M. Munye, A.D. Tagalakis, M.D.I. Manunta, S.L. Hart, The role of the  
459 helper lipid on the DNA transfection efficiency of lipopolyplex formulations, *Sci.*  
460 *Rep.* 4 (2014) 7107.

- 461 20. D.W. Malcolm, J.J. Varghese, J.E. Sorrells, C.E. Ovitt, D.S.W. Benoit, The effects  
462 of biological fluids on colloidal stability and siRNA delivery of a pH-responsive  
463 micellar nanoparticle delivery system, *ACS Nano* 12 (2018) 187–197.
- 464 21. Y. Sakurai, W. Mizumura, K. Ito, K. Iwasaki, T. Katoh, Y. Goto, H. Suga, H.  
465 Harashima, Improved stability of siRNA-loaded lipid nanoparticles prepared with a  
466 PEG-monoacyl fatty acid facilitates ligand-mediated siRNA delivery, *Mol. Pharm.*  
467 17 (2020) 1397-1404.
- 468 22. C. Madeira, L.M.S. Loura, M. Prieto, A. Fedorov, M.R. Aires-Barros, Effect of  
469 ionic strength and presence of serum on lipoplexes structure monitorized by FRET,  
470 *BMC Biotechnol.* 8 (2008) 20.
- 471 23. M. Scarzello, V. Chupin, A. Wagenaar, M.C.A. Stuart, J.B.F.N. Engberts, R. Hulst,  
472 Polymorphism of pyridinium amphiphiles for gene delivery: influence of ionic  
473 strength, helper lipid content, and plasmid DNA complexation, *Biophys. J.* 88  
474 (2005) 2104-2113.
- 475 24. H. Kang, S. Rho, W.R. Stiles, S. Hu, Y. Baek, D.W. Hwang, S. Kashiwagi, M.S.  
476 Kim, H.S. Choi, Size-dependent EPR effect of polymeric nanoparticles on tumor  
477 targeting, *Adv. Healthc. Mater.* 9 (2020) e1901223.

- 478 25. A. Nel, E. Ruoslahti, H. Meng, New insights into "permeability" as in the enhanced  
479 permeability and retention effect of cancer nanotherapeutics, *ACS Nano* 11 (2017)  
480 9567-9569.
- 481 26. S. Zhang, J. Li, G. Lykotrafitis, G. Bao, S. Suresh, Size-dependent endocytosis of  
482 nanoparticles, *Adv. Mater.* 21 (2009) 419–424.
- 483 27. J. Rejman, V. Oberle, I.S. Zuhorn, D. Hoekstra, Size-dependent internalization of  
484 particles via the pathways of clathrin- and caveolae-mediated endocytosis, *Biochem.*  
485 *J.* 377 (2004) 159-169.
- 486 28. P. Das, N.R. Jana, Highly colloidally stable hyperbranched polyglycerol grafted red  
487 fluorescent silicon nanoparticle as bioimaging probe, *ACS Appl. Mater. Interfaces* 6  
488 (2014) 4301-4309.
- 489 29. H.-Z. Jia, W. Zhang, J.-Y. Zhu, B. Yang, S. Chen, G. Chen, Y.-F. Zhao, J. Feng, X.-  
490 Z. Zhang, Hyperbranched-hyperbranched polymeric nanoassembly to mediate  
491 controllable co-delivery of siRNA and drug for synergistic tumor therapy, *J.*  
492 *Control. Release* 216 (2015) 9-17.
- 493 30. N.D. Santos, C. Allen, A.-M. Doppen, M. Anantha, K.A.K. Cox, R.C. Gallagher, G.  
494 Karlsson, K. Edwards, G. Kenner, L. Samuels, et al., Influence of poly(ethylene  
495 glycol) grafting density and polymer length on liposomes: relating plasma

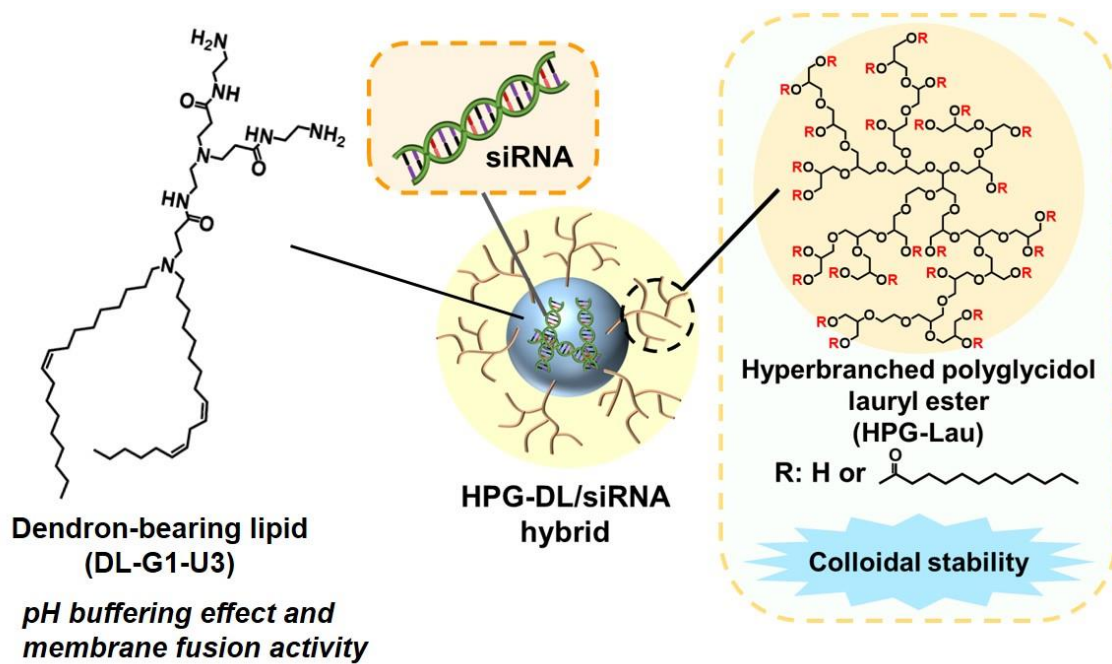
496 circulation lifetimes to protein binding, *Biochim. Biophys. Acta* 1768 (2007) 1367-  
497 1377.

498 31. Y. Hattori, K. Tamaki, S. Sakasai, K.-I. Ozaki, H. Onishi, Effects of PEG anchors in  
499 PEGylated siRNA lipoplexes on *in vitro* gene-silencing effects and siRNA  
500 biodistribution in mice, *Mol. Med. Rep.* 22 (2020) 4183–4196.

501 32. K. Hashiba, Y. Sato, H. Harashima, pH-labile PEGylation of siRNA-loaded lipid  
502 nanoparticle improves active targeting and gene silencing activity in hepatocytes, *J.*  
503 *Control. Release* 262 (2017) 239-246.

504 33. H. Hatakeyama, H. Akita, H. Harashima, A multifunctional envelope type nano  
505 device (MEND) for gene delivery to tumours based on the EPR effect: a strategy for  
506 overcoming the PEG dilemma, *Adv. Drug Deliv. Rev.* 63 (2011) 152-160.  
507

508 TOC image:



509

510